

# A 38 $\mu$ A Wearable Biosignal Monitoring System with Near Field Communication

Ken Yamashita<sup>1</sup>, Shintaro Izumi<sup>1</sup>, Masanao Nakano<sup>1</sup>, Takahide Fujii<sup>1</sup>, Toshihiro Konishi<sup>1</sup>, Hiroshi Kawaguchi<sup>1</sup>, Hiromitsu Kimura<sup>2</sup>, Kyoji Marumoto<sup>2</sup>, Takaaki Fuchikami<sup>2</sup>, Yoshikazu Fujimori<sup>2</sup>, Hiroshi Nakajima<sup>3</sup>, Toshikazu Shiga<sup>4</sup>, and Masahiko Yoshimoto<sup>1,5</sup>

<sup>1</sup>Kobe University, Kobe, Japan, <sup>2</sup>Rohm Co. Ltd., Kyoto, Japan, <sup>3</sup>Omron Corp., Kyoto, Japan,

<sup>4</sup>Omron Healthcare Inc., Kyoto, Japan, <sup>5</sup>JST CREST, Tokyo, Japan

E-mail: yamashita@cs28.cs.kobe-u.ac.jp

**Abstract**—This paper presents a low-power wearable biosignal monitoring system. The proposed system can communicate with smartphones using Near Field Communication (NFC) to check vital signs easily at any time. It comprises a battery, electrodes, a triaxial accelerometer IC, an NFC tag IC, and a biosignal processor LSI. The proposed biosignal processor LSI, fabricated using a 130-nm CMOS process, comprises heart rate monitoring circuits, a 32-kbyte ferroelectric random access memory (FeRAM), an accelerometer interface, and an NFC interface. The proposed system consumes 38.1  $\mu$ A for logging application at 32-kHz operating frequency, with 3.0-V supply voltage.

## I. INTRODUCTION

Mobile health is expected to play an increasingly prominent role in health provision because of the advent of an aging society [1]. Especially, daily life monitoring is important to prevent lifestyle diseases, which are expected to raise the number of patients and elderly people who need nursing care. Our goal is to monitor and display vital signals and physical activity in daily life to improve users' quality of life and to realize a smart society.

This report specifically describes a wearable biosignal monitoring system, which can acquire long-term instantaneous heart rate (IHR) data and an acceleration value. The physical activities in daily life (e.g., locomotive, household activities) are classifiable using a triaxial accelerometer [2]. The IHR, which is calculated from the interval of R-waves in electrocardiogram (ECG), is useful for heart disease detection, heart rate variation (HRV) analysis [3], and exercise intensity estimation [4]. The key factors affecting wearable system usability are miniaturization and weight reduction. Battery mass and power consumption must be reduced because battery mass dominates wearable systems. Therefore, the main purpose of our research is power reduction.

## II. SYSTEM DESIGN

Fig. 1 presents an illustration of an overview of the wearable biosignal monitoring system. The paste-type biosignal sensor comprises a battery, electrodes, a triaxial accelerometer IC, a near field communication (NFC) tag IC, and a biosignal processor LSI. An application on the

smartphone provides parameter configuration and data retrieval functions using NFC. Using it, a user can easily check vital signs at any time.

To minimize biosignal acquisition power consumption, we developed a biosignal processor LSI. Fig. 2 depicts the block diagram of proposed biosignal processor LSI. It comprises a heart rate monitor, 32-kbyte ferroelectric random access memory (FeRAM), an accelerometer interface, and an NFC interface.

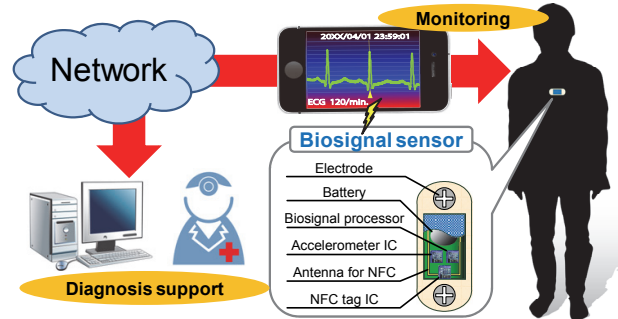


Figure 1. Wearable biosignal monitoring system overview.

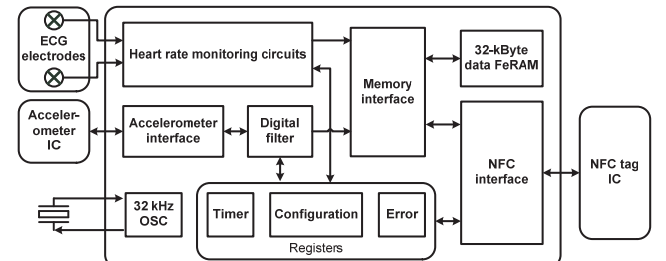


Figure 2. Block diagram of proposed biosignal processor LSI.

### A. Biosignal Monitoring and Data Logging

The biosignal processor LSI acquires an acceleration value from off-chip triaxial accelerometer IC and IHR from heart-rate monitoring circuits. These values are stored in a data buffer until they are retrieved by a smartphone. The frequency range of biosignals is low (less than 1 kHz). Therefore, the

\*Research supported by Ministry of Economy, Trade and Industry (METI) and the New Energy and Industrial Technology Development Organization (NEDO).

required active ratio of biosignal monitoring system is small. The standby current of the data buffer should therefore be reduced. We used FeRAM because it is non-volatile memory and because it does not consume standby current.

Fig. 3 presents an illustration of the heart rate monitor. First, the ECG signal is amplified by an instrumental amplifier and an operational amplifier. Then, an R-wave pulse is generated by a peak-hold circuit and a comparator. An IHR calculator detects the rising edge of R-wave pulse and calculates the IHR. Fig. 4 presents the calculation flow of IHR. Here,  $IHR[n]$  is the output value of IHR calculator. The variable  $t_1$  and  $t_2$  store the TIMER value. If calculated IHR does not satisfy the following conditions, then is treated as an error.

- a) IHR is greater than 273 ms
- b) IHR is less than 2000 ms
- c) IHR variation from the prior value is smaller than  $\pm 25\%$

Constraint c) is applied only when the prior IHR, as calculated using the prior R-wave, is not an error value. The output values of IHR calculator will not be updated. An error flag register is set if the error occurs.

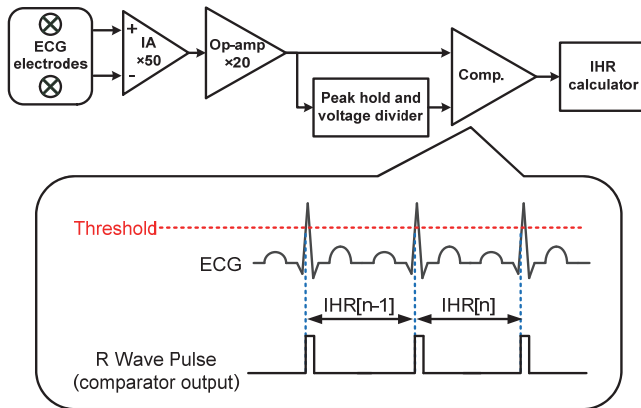


Figure 3. Heart rate monitoring circuits.

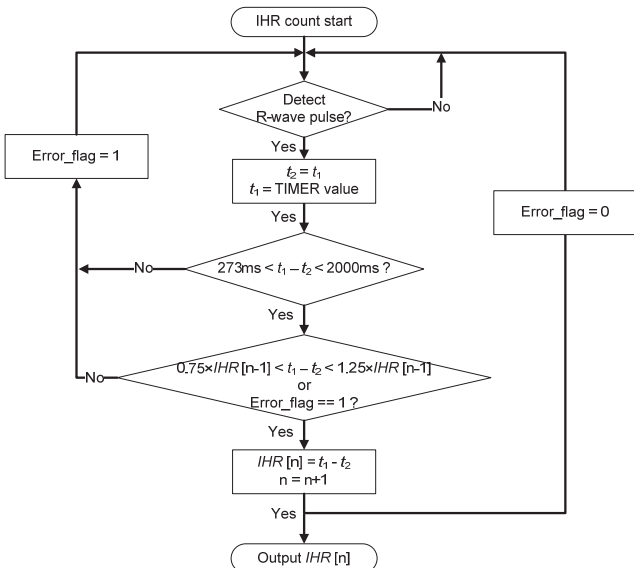


Figure 4. Calculation flow of the IHR.

## B. Data Communication

The proposed system uses NFC to cooperate with smartphone (or a reader/writer). Several smartphones and tablet devices now support NFC technology.

Generally, a wireless transceiver consumes the greatest amount of power in the biosignal monitoring system. However, compared with Bluetooth Low Energy or ZigBee, the standby power of NFC is extremely small. Moreover, the active communication energy is only consumed on the reader/writer side when using a passive mode, in which only the initiator generates a carrier during communications [5]. In addition, NFC enables us to initiate communication without manually configuring the communication link, unlike Bluetooth [6]. The NFC also has high security because it has a short communication range. Some secure payment services already use NFC [6].

Fig. 5 portrays the communication sequences of parameter configuration and data retrieval. To configure the parameters, the NFC controller can update the configuration registers. The logging data can be retrieved directly from the data buffer. The user can also read the parameter setting and timer value from configuration registers and timer. The logging start, logging stop, and system reset command are also issued from a smartphone.

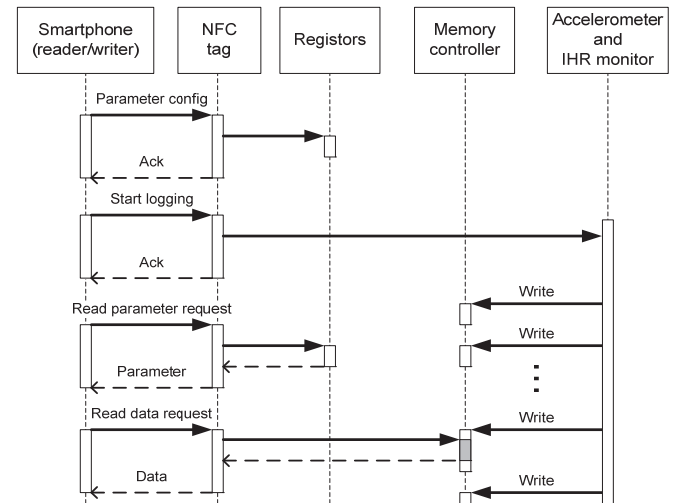


Figure 5. Operation sequences.

## III. VLSI IMPLEMENTATION AND MEASUREMENT RESULTS

Fig. 6 shows the biosignal processor LSI, which is fabricated in 130 nm CMOS technology. It consumes 13.1  $\mu$ A, on average, in data logging operation with 32-kHz operating frequency and 3.0 V supply voltage. Then, the IHR value and acceleration value are stored to FeRAM every second. Fig. 7 presents a photograph of our developed paste-type biosignal sensor, which has  $28 \times 35 \times 9$  mm<sup>3</sup> volume and 3.6 g weight including a battery. To demonstrate its operations using NFC, we built an Android application, as presented in Fig. 8. The left side of Fig. 8 shows a screen shot of the parameter configuration. The right side shows a screen shot of the obtained data. The required communication times for

parameter configuration and 32-kbyte data retrieval are 1 s and 35 s, respectively.

Figs. 9 and 10 show the time series variation of current consumption and the breakdown of average current consumption, which include the biosignal processor LSI, the NFC tag IC, and the accelerometer IC. Then the sampling rate of acceleration values is set to 32 S/s. At the system level, the average current consumption is 12.2  $\mu$ A at standby, 38.1  $\mu$ A at data logging, and 645  $\mu$ A at data communication. Although data communication consumes a great amount of power because we use an active NFC tag [7] in this experiment, it will be reduced by replacing the active tag to a passive tag in future work. Table I presents a performance comparison between the proposed circuit and those of earlier works. Table I shows the benefit of this work: low power consumption.

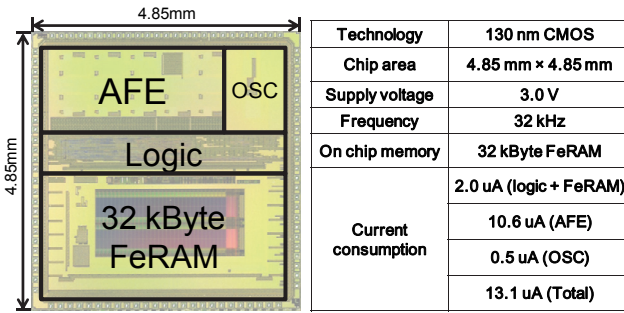


Figure 6. Chip photograph and specification of biosignal processor LSI.

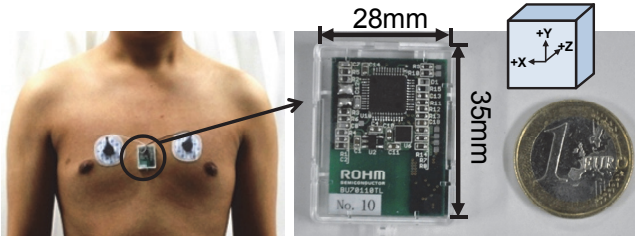


Figure 7. Prototype of a biosignal sensor.

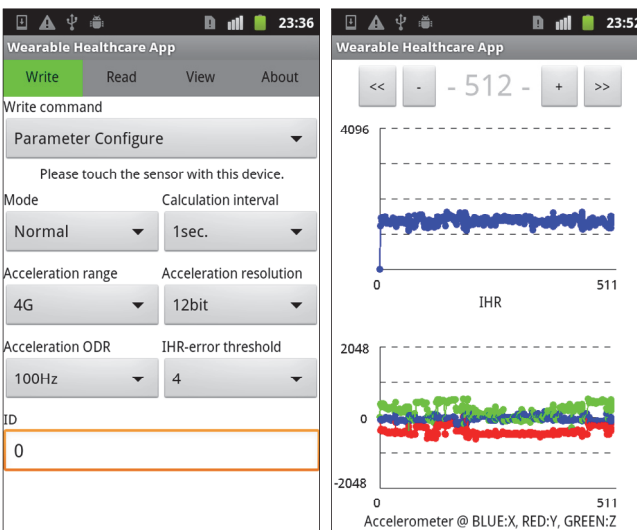


Figure 8. Screen shots of the Android application.

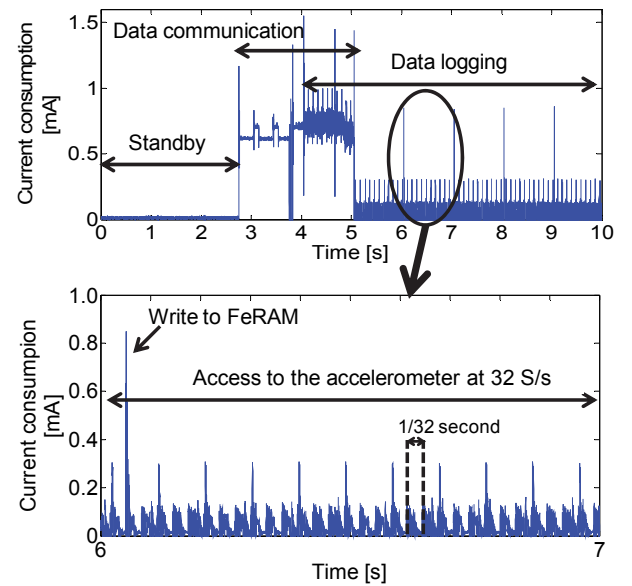


Figure 9. Time series variation of system-level current consumption.

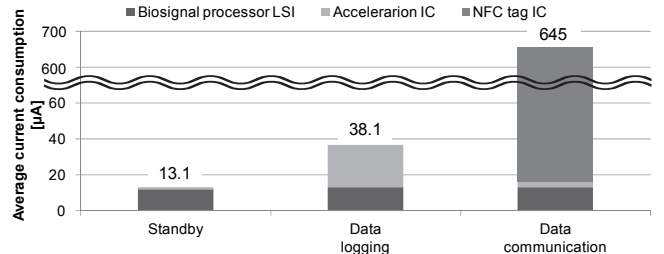


Figure 10. Breakdown of average current consumption.

Next, we evaluated long-term data logging with a healthy subject, a 23-year-old man, in daily life. The upper side of Fig. 11 shows the obtained acceleration value. The bottom side shows the heart rates calculated from the obtained IHR. Our biosignal sensor is not waterproof. Therefore, the sensor is removed during bath time. Although several errors are included in the obtained IHR data, almost all errors can be corrected from prior IHR values or subsequent IHR values.

Finally, we verified the noise tolerance of proposed system using a clean ECG waveform of the MIT-BIH Arrhythmia Database (#100) [10] and a muscle artifact noise waveform of MIT-BIH Noise Stress Test Database [11]. According to the definition in [11], we organized the noisy ECG waveforms with 15, 14, and 13 dB signal-to-noise ratio (SNR). These waveforms are generated from a signal generator as presented in Fig. 12. Then we evaluated the accuracy of IHR output. Fig. 13 shows the measurement result of noise stress test. When SNR is lower than 14 dB, the obtained IHR of the proposed biosignal sensor is affected by noise. The root mean square errors of IHR at 15, 14, and 13 dB SNR are, respectively,  $7.0 \times 10^{-5}$ ,  $1.0 \times 10^{-2}$ , and  $6.0 \times 10^{-2}$ .

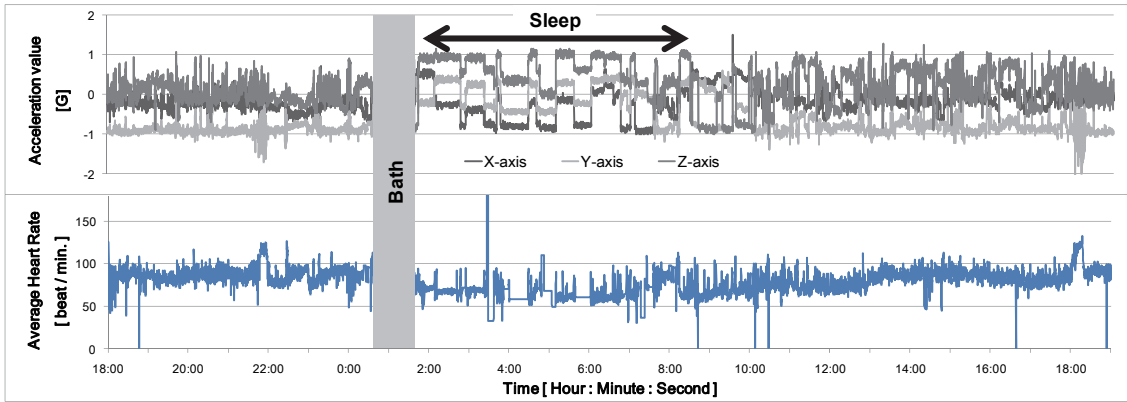


Figure 11. Measurement results of Daily life monitoring.



Figure 12. Noise stress test environment.

TABLE I. PERFORMANCE COMPARISON

	This Work	Dinh et al. [8]	Yamakawa et al. [9]
Technology	130 nm	Discrete	350 nm
Supply voltage	3.0 V	3.7 V	2.6–3.3V
Current	38.1 $\mu$ A	3 mA	212 $\mu$ A
Sensor	Acceleration/ Electrodes	Microphone	Microphone / Pressure sensor/ Electrodes
Communication	NFC	Zigbee	RFID

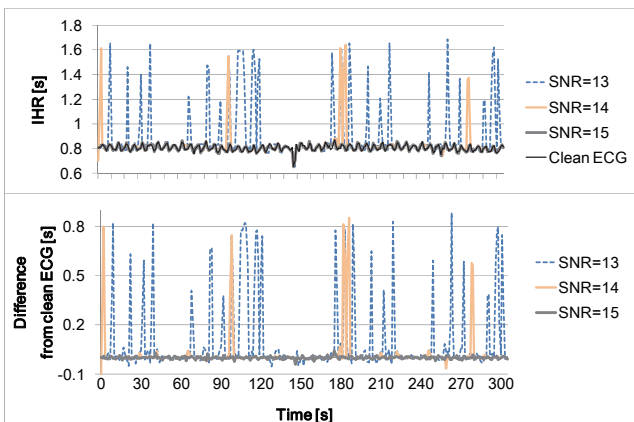


Figure 13. Measurement results of noise stress test.

#### IV. CONCLUSION

As described in this paper, we examined a wearable biosignal monitoring system that can acquire acceleration and IHR data. We developed a prototype system using the proposed biosignal processing LSI, which can communicate with the Android application by NFC. The average power consumption during data logging was 38.1  $\mu$ A, including the proposed biosignal processing LSI, the NFC tag IC, and accelerometer IC. The noise tolerance of the proposed system is evaluated. It correctly functioned at SNR higher than 15-dB.

#### REFERENCES

- [1] H. Nakajima, T. Shiga, and Y. Hara, "Systems Health Care," In Proc. of IEEE SMC, pp. 1167-1172, Oct. 2011.
- [2] Y. Oshima, K. Kawaguchi, S. Tanaka, K. Ohkawara, Y. Hikihara, K. Ishikawa-Tanaka, and I. Tabata, "Classifying household and locomotive activities using a triaxial accelerometer," Gait and Posture, vol. 31, pp. 370-374, 2010.
- [3] W. Roel and M. John, "Comparing Spectra of a series of Point Events Particularly for Heart Rate Variability Data," IEEE T-BME, BME-31, no.4, pp.384-387, Apr. 1984.
- [4] S. Yazaki and T. Matsunaga, "Evaluation of activity level of daily life based on heart rate and acceleration," In Proc. of SICE, pp. 1002-1005, Aug. 2010.
- [5] E. Strommer, J. Kaartinen, J. Parkka, A. Ylisaukko-oja, and I. Korhonen, "Application of Near Field Communication for Health Monitoring in Daily Life," In Proc. of IEEE EMBS, pp. 3246-3249, Aug. 2006.
- [6] J. Morak, H. Kumpusch, D. Hayn, R. Modre-Osprian, and G. Schreier, "Design and Evaluation of a Telemonitoring Concept Based on NFC-Enabled Mobile Phones and Sensor Devices," IEEE T-ITB, vol. 16, no. 1, pp. 17-23, 2012.
- [7] Felica Contactless IC Card Technology, "<http://www.sony.net/Products/felica/>"
- [8] A. Dinh and T. Wang, "Bandage-Size Non-ECG Heart Rate Monitor Using ZigBee Wireless Link," ICBBT, pp. 160-163, 2010.
- [9] T. Yamakawa, T. Inoue, M. Harada, and A. Tsuneda, "Design of a CMOS Heartbeat Spike-Pulse Detection Circuit Integrable in an RFID Tag for Heart Rate Signal Sensing," IEICE Trans. Electron., vol. E90-C, no. 6, 2007.
- [10] MIT-BIH Arrhythmia Database (mitdb), Record 100, "<http://www.physionet.org/physiobank/database/mitdb/>"
- [11] MIT-BIH Noise Stress Test Database (nstdb), "<http://www.physionet.org/physiobank/database/nstdb/>"